Available online at www.sciencedirect.com

ScienceDirect

Journal of Organometallic Chemistry 692 (2007) 4161–4167

Journal of Organo metallic Chemistry

www.elsevier.com/locate/jorganchem

A novel tricarbonyl rhenium complex of 2-benzoylpyridine – Synthesis, spectroscopic characterization, X-ray structure and DFT calculations

B. Machura [a,*], R. Kruszynski [b]

[a] *Department of Crystallography, Institute of Chemistry, University of Silesia, 9th Szkolna St., 40-006 Katowice, Poland*
[b] *Department of X-ray Crystallography and Crystal Chemistry, Institute of General and Ecological Chemistry, Technical University of Lodz, 116 Żeromski St., 90-924 Łódź, Poland*

Received 11 April 2007; received in revised form 14 June 2007; accepted 19 June 2007
Available online 29 June 2007

Abstract

The reaction of $Re(CO)_5Cl$ with 2-benzoylpyridine (bopy) has been examined and a novel $Re(CO)_3{}^+$ tricarbonyl – *fac*-$[Re(CO)_3(bopy)Cl]$ – has been obtained. The compound has been studied by IR, UV–Vis spectroscopy and X-ray crystallography. The molecular orbital diagram of the tricarbonyl has been calculated with the density functional theory (DFT) method. The spin-allowed singlet–singlet electronic transitions of $[Re(CO)_3(bopy)Cl]$ have been calculated with the time-dependent DFT method, and the UV–Vis spectrum of the title compound has been discussed on this basis.

Keywords: Rhenium(I) carbonyl complexes; X-ray structure; UV–Vis spectra; DFT calculations

1. Introduction

The d^6 transition metal complexes with heteroaromatic ligands have been the subject of intense investigations for many years. The interest of researches has been attracted mostly by their unique photophysical and photochemical properties, crucial for numerous potential and already introduced practical applications. The most frequently studied compounds of this type are complexes of general formula *fac*-$[Re(CO)_3(L–L)(E)]^{0/+}$, where E stands for a halogen atom or other ligand approximately axial to the heteroaromatic rings plane. The photobehaviour of such complexes may be discussed in terms of three types of excited states: (i) metal-to-ligand charge transfer (MLCT) states, (ii) ligand-to-ligand charge transfer (LLCT) states, (iii) intraligand (IL) states. The latter one appears to lie at rather high energies in the *fac*-$[Re(CO)_3(L–L)(E)]^{0/+}$ complexes, and they are of little photochemical importance. The excited states of $[Re(CO)_3(L–L)(E)]^{0/+}$ complexes are often sufficiently long-lived to become engaged in energy transfer reactions. Currently, several *fac*-$Re(CO)_3{}^+$ complexes are used as electroluminescent materials in OLED-type devices [1–12].

Furthermore, the excited states of $[Re(CO)_3(L–L)(E)]^{0/+}$ complexes may be both strong reductants and oxidants. The high reactivity of the reduced species may be utilized in photocatalysis. For example, photoexcitation of $[Re(CO)_3(bipy)Cl]$ in the presence of triethylamine produces $[Re(CO)_3(bipy)Cl]^-$, which loses the chloride ligand. The further reaction with CO_2 results in the photocatalytic CO_2 reduction to CO [10].

The spectroscopic and redox behaviour of the Re(I) complexes are ligand dependent and can be tuned by varying the identity of their chelate ligands, so there is a clear need to synthesize and investigate novel species of this type.

---

[*] Corresponding author.
E-mail addresses: basia@ich.us.edu.pl (B. Machura), rafal.kruszynski@p.lodz.pl (R. Kruszynski).

0022-328X/$ - see front matter © 2007 Elsevier B.V. All rights reserved.
doi:10.1016/j.jorganchem.2007.06.036

Here, we present the synthesis, spectroscopic characterization, crystal and molecular structure of the *fac*-[Re(CO)$_3$(bopy)Cl] (**1**) tricarbonyl with 2-benzoylpyridine (bopy). The binding of bopy to the central ion occurs through the N–O chelating site. This coordination produces a five-membered ring containing an unsaturated α-iminoketo function which can act as a π acceptor towards a bound π electron-rich metal center such as rhenium(I). The α-iminoketo chelation plays an important role in the biosynthesis of the pterins, lumazines, flavins coenzymes [13,14]. Accordingly, the complex **1** may be viewed as a simple model for such metalloenzymes.

The molecular orbital diagram of **1** has been calculated with the density functional theory (DFT) calculations. Currently, the DFT method is commonly used to examine the electronic structure of transition metal complexes. It meets with the requirements of being accurate, easy to use and fast enough to allow the study of relatively large molecules of transition metal complexes [15]. The spin-allowed singlet–singlet electronic transitions of **1** have been calculated with the time-dependent DFT method (TDDFT method), and a good assignment with the experimental spectrum has been observed.

2. Experimental

2.1. General procedure

The reaction was performed under an argon atmosphere. The solvents were dried before use, using the appropriate drying reagents. Re(CO)$_5$Cl and bopy were purchased from Aldrich, and used as received.

The IR spectrum was recorded on a Nicolet Magna 560 spectrophotometer in the spectral range 4000–400 cm^{-1} with the samples in the form of KBr pellets. The electronic spectrum was measured on a spectrophotometer Lab Alliance UV–Vis 8500 in the range 1000–200 nm in dichloromethane solution. Elemental analyses (C H N) were performed on a Perkin–Elmer CHN-2400 analyzer.

2.2. Preparation of [Re(CO)$_3$(bopy)Cl] (1)

Re(CO)$_5$Cl (0.2 g, 0.55 mmol) and bopy (0.11 g, 0.60 mmol) in toluene (80 cm^3) were refluxed for 6 h. The resulting reaction mixture was allowed to cool to room temperature and reduced in volume to ~10 ml. An off-red solid was filtered off, washed with hexane, diethyl ether, and dried; yield 85%. Single crystals of complex **1** were grown by the slow diffusion of diethyl ether into a solution of the complex dissolved in dichloromethane.

IR (KBr, cm^{-1}): ν_{CO} = 2027, 1920, 1863 and 1672 cm^{-1}; ν_{CN} and $\nu_{C=C}$ = 1593, 1572 and 1552 cm^{-1}. (Calc. for $C_{15}H_9ClNO_4Re$: C, 36.85; H, 1.86; N, 2.86. Found: C, 36.76; H, 1.90; N, 2.79%).

Table 1
Crystal data and structure refinement for **1**

Empirical formula	$C_{15}H_9ClNO_4Re$
Formula weight	488.88
Temperature (K)	291.0(3)
Wavelength (Å)	0.71073
Crystal system	Monoclinic
Space group	$P2_1/c$
Unit cell dimensions	
a (Å)	15.3719(6)
b (Å)	11.4640(5)
c (Å)	8.3746(4)
β (°)	93.555(4)
Volume (Å^3)	1472.96(11)
Z	4
D_{calc} (Mg/m^3)	2.205
Absorption coefficient (mm^{-1})	8.447
$F(000)$	920
Crystal size (mm)	0.462 × 0.266 × 0.264
θ Range for data collection (°)	2.66–25.00
Index ranges	$-17 \leqslant h \leqslant 18$, $-13 \leqslant k \leqslant 13$, $-8 \leqslant l \leqslant 9$
Reflections collected	15203
Independent reflections (R_{int})	2584 (0.0424)
Completeness to 2θ (%)	99.9
Maximum and minimum transmission	0.111 and 0.082
Data/restraints/parameters	2584/0/199
Goodness-of-fit on F^2	1.073
Final R indices [$I > 2\sigma(I)$]	$R_1 = 0.0295$, $wR_2 = 0.0745$
R indices (all data)	$R_1 = 0.0354$, $wR_2 = 0.0797$
Largest difference in peak and hole (e Å^{-3})	1.181 and −1.222

2.3. Crystal structures determination and refinement

The yellow crystal of **1** was mounted on a KM-4-CCD automatic diffractometer equipped with a CCD detector, and used for data collection. X-ray intensity data were collected with graphite monochromated Mo Kα radiation ($\lambda = 0.71073$ Å) at temperature of 291.0(3) K, with ω scan mode. Details concerning crystal data and refinement are given in Table 1. Lorentz, polarization and empirical absorption corrections [16] were applied. The structure was solved by the Patterson method and subsequently completed by the difference Fourier recycling. All the non-hydrogen atoms were refined anisotropically using full-matrix, least-squares technique. The hydrogen atoms were treated as "riding" on their parent carbon atoms [$d(C\cdots H) = 0.93$ Å] and assigned isotropic temperature factors equal 1.2 times the value of equivalent temperature factor of the parent carbon atom. SHELXS97 [17], SHELXL97 [18] and SHELXTL [19] programs were used for all the calculations. Atomic scattering factors were those incorporated in the computer programs.

3. Computational details

GAUSSIAN03 program [20] was used in the calculations. The geometry of **1** was optimized in the singlet state with the DFT method with the use of B3LYP functional [21,22]. The electronic spectrum of **1** was calculated with the TDDFT method [23]. The solvent effect was simulated using the polarizable continuum model (PCM) in which the solvent cavity is seen as a union of interlocking atomic spheres. The calculations were performed by using ECP basis set on the rhenium atom, and the standard 6-31G basis set for others. For chloride, oxygen, phosphorous and nitrogen atoms, diffuse and polarization functions were added [24,25]. The Xe core electrons of Re were replaced by an effective core potential and DZ quality Hay and Wadt Los Alamos ECP basis set (LANL2DZ) [26] was used for the valence electrons. Additional d function with exponent $\alpha = 0.3811$ and f function with exponent $\alpha = 2.033$ on the rhenium atom were added [27].

4. Results and discussion

4.1. Preparation and Infrared data

The title complex was prepared by refluxing of $[Re(CO)_5Cl]$ with a small excess of 2-benzoylpyridine in toluene. It was isolated as air-stable, microcrystalline solid, soluble in common organic solvents. The infrared spectrum of **1** displays three bands in the carbonyl stretching region: a sharp intense band at 2027 cm^{-1} and two lower-energy bands 1920 and 1863 cm^{-1}. This pattern corresponds to three CO units in a *fac* isomer arrangement [28]. A band due to the bopy ν(C=O) vibration appears at 1672 cm^{-1}, and characteristic bands of the C=C and C=N stretching modes of 2-benzoylpyridine are observed in the range 1600–1550 cm^{-1} [29].

4.1.1. Crystal structure

The crystallographic data for the title complex are given in Table 1. The perspective drawing of **1** with atomic numbering is shown in Fig. 1. The overall structure of **1** can be considered as a distorted octahedral with the largest deviations from the expected 90° bond angles coming from the bite angle of 2-benzoylpyridine. It equals to 73.9(1)°, and it is similar to that reported for the related $[Re(CO)_3(6\text{-ATML})Cl] \cdot 3C_6H_6$ (6-ATML = 6-acetyl-1,3,7-trimethyllumazine) [75.2(1)°]. The bite angles O–M–N in the structures with α-iminoketo chelate ligands bounded to transition metals depend mainly on the size of the metal center, the smallest values (down to 67°) were found for Ag^I complexes and the largest angles (up to 85°) were observed for compounds with Cu^{II}[13].

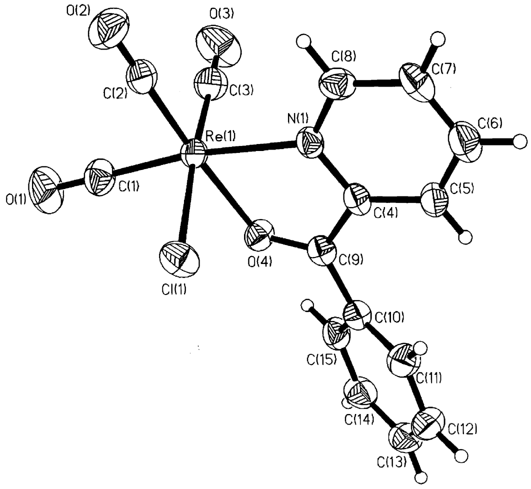

Fig. 1. Molecular structure of **1**.

Table 2
The experimental and optimized bond lengths [Å] and angles [°] for **1**

	Bond lengths			Bond angles	
	Experimental	Optimized		Experimental	Optimized
Re(1)–C(1)	1.931(7)	1.937	C(2)–Re(1)–C(1)	87.7(2)	90.32
Re(1)–C(2)	1.898(6)	1.913	C(2)–Re(1)–C(3)	90.7(3)	90.77
Re(1)–C(3)	1.931(7)	1.921	C(3)–Re(1)–C(1)	90.3(3)	90.85
Re(1)–Cl(1)	2.458(1)	2.517	C(2)–Re(1)–O(4)	172.0(2)	170.88
Re(1)–N(1)	2.181(5)	2.202	C(3)–Re(1)–O(4)	93.3(2)	94.84
Re(1)–O(4)	2.149(3)	2.179	C(1)–Re(1)–O(4)	99.1(2)	96.77
C(1)–O(1)	1.130(8)	1.157	C(2)–Re(1)–N(1)	99.0(2)	99.35
C(2)–O(2)	1.142(7)	1.162	C(3)–Re(1)–N(1)	94.2(2)	94.57
C(3)–O(3)	1.106(8)	1.165	C(1)–Re(1)–N(1)	171.8(2)	168.83
C(9)–O(4)	1.246(6)	1.249	O(4)–Re(1)–N(1)	73.9(1)	73.07
			C(2)–Re(1)–Cl(1)	94.7(2)	91.77
			C(3)–Re(1)–Cl(1)	174.5(2)	176.06
			C(1)–Re(1)–Cl(1)	91.0(2)	92.14
			O(4)–Re(1)–Cl(1)	81.12(1)	82.27
			N(1)–Re(1)–Cl(1)	83.9(1)	82.05
			O(1)–C(1)–Re(1)	178.7(5)	178.06
			O(2)–C(2)–Re(1)	177.5(6)	177.18
			O(3)–C(3)–Re(1)	178.7(6)	179.40

The electron-rich central ion of **1** shows larger affinity towards the less basic but strongly π accepting carbonyl oxo atom, and the Re–O(4) is slightly shorter than the Re–N(1) bond (Table 2). The value $\Delta = d(\text{M–N}) - d(\text{M–O})$, reflecting the symmetry of the chelate arrangement in such structures, is equal to 0.032 Å for **1**. It can be assumed that the Re center is situated symmetrically between N(1) and O(4) donor atoms.

The pyridyl and phenyl substituents of bopy ligand are planar in the range of experimental error and they are inclined at 40.1(2)°. The aromatic rings: pyridyl···pyridyl# (x, $-y+1.5$, $z-0.5$), pyridyl···pyridyl# (x, $-y+1.5$, $z+0.5$), phenyl···phenyl ($-x+1$, $-y+1$, $-z$) are connected via π···π stacking interactions [30]. The distances between ring centroids are equal to 4.204(9), 4.204(9), 3.618(9) Å respectively, and the dihedral angles between the rings are following 7.4(6)°, 7.4(6)°, 0.0(7)°. The angles between linking ring centroids vector and normal to the first of stacked rings are equal to 36.4(6)°, 35.3(6)°, 20.0(7)°, whereas the perpendicular distances between first

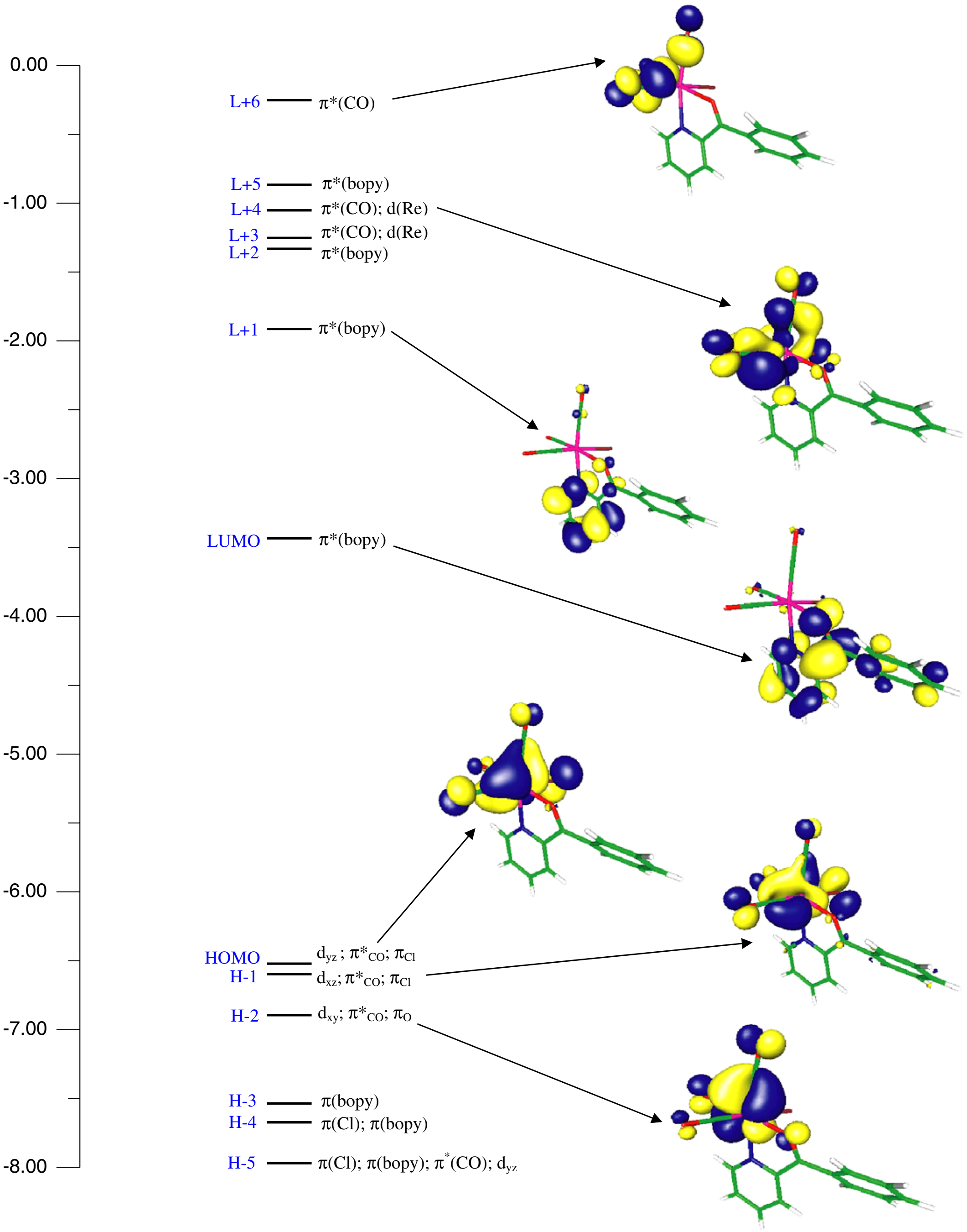

Fig. 2. The energy (eV), character and some contours of the occupied and unoccupied molecular orbitals of **1**.

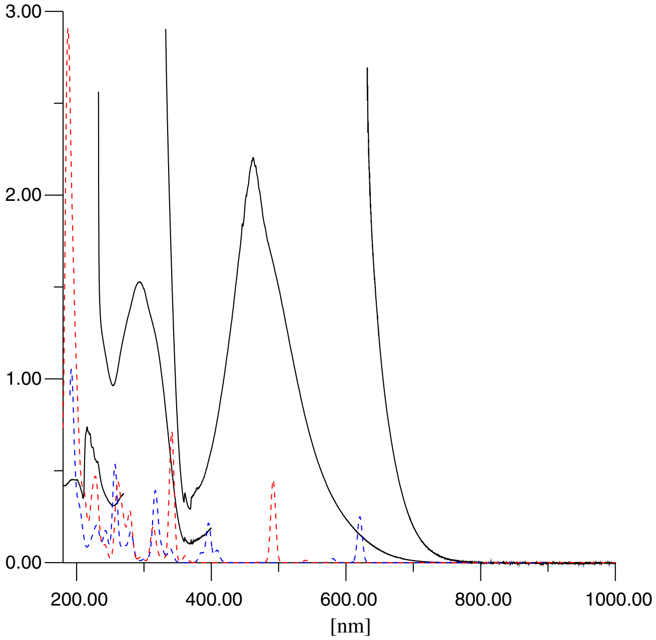

Fig. 3. The experimental and calculated electronic absorption spectra of **1**. Full line: the experimental spectrum measured in CH_2Cl_2. Blue dashed line: spectrum calculated in vacuum. Red dashed line: spectrum calculated in dichloromethane. (For interpretation of the references in colour in this figure legend, the reader is referred to the web version this article.)

of stacked rings centroid and second ring are 3.430(9), 3.382(9), 3.400(9) Å.

4.1.2. Optimized geometry

The geometry of **1** was optimized in a singlet state by the DFT method with the B3LYP functional. The optimized geometric parameters are gathered in Table 2. The calculated bond lengths and angles are in agreement with the values based upon the X-ray crystal structure data, and the general trends observed in the experimental data are well reproduced in the calculations.

4.1.3. Electronic structure

The complex **1** is a closed-shell structure. Its molecular orbital diagram with several occupied and virtual molecular orbital contours is presented in Fig. 2. The HOMO–LUMO gap equals to 3.09 eV. The low-lying virtual orbitals correspond mainly to π^*_{bopy} and π^*_{CO}. The LUMO, LUMO + 1, LUMO + 2 and LUMO + 5 are centered on the bopy ligand. The higher virtual orbitals are delocalized among Re and carbonyls or among Re, carbonyls and bopy.

The three highest occupied molecular orbitals are predominately localized on the rhenium atom, corresponding to the $(5d_{xy})^2(5d_{xz})^2\ (5d_{yz})^2$ occupation of the central ion. However, ligand contributions are also important. All these orbitals have a relatively considerable CO character. The HOMO and HOMO − 1 orbitals contain an admixture of chloride p_π orbitals, and HOMO − 2 – admixture of π oxygen orbital of bopy ligand.

4.2. Electronic spectrum

The electronic absorption spectrum was measured at room temperature in dichloromethane, and the experimental absorption bands were assigned using the singlet excited states calculated with the time-dependent DFT method. The experimental and calculated electronic spectra of **1** are compared in Fig. 3. Each calculated transition is represented by a gaussian function $y = ce^{-bx^2}$ with the height (c) equal to the oscillator strength and b equal to 0.04 nm^{-2}. As seen in Fig. 3, TDDFT/PCM calculations well reproduce the absorption spectrum of **1** measured in dichloromethane. The lowest allowed absorption band, which occurs at 2.55 eV, has been calculated at 2.29 eV. The agreement between the experimental and calculated spectra is worse when the solvent is neglected. Neglecting the solvent strongly underestimates energies of the low-lying electronic transitions. The lowest absorption band energy is underestimated by 0.55 eV in this case.

Table 3 shows the spin-allowed singlet–singlet electronic transitions calculated with the TDDFT method for **1**. For the high energy part of the spectrum, only transitions with oscillator strengths larger than 0.020 are listed in Table 3. The assignment of the calculated transitions to the experimental bands is based on the criterion of the energy and oscillator strength of the calculated transitions.

The low-energy absorption band of 1.246(6) **1** appears at 466.3 nm, and is red shifted in comparison with the longest wavelength experimental band (370 nm) of $[Re(CO)_3(bipy)Cl]$ [7]. The TDDFT/PCM calculations show that it originates predominately in the HOMO − 1 → LUMO transition. As can be seen from Fig. 2, the HOMO − 1 is delocalized on the whole $Re(CO)_3Cl$ unit, and the LUMO is completely centered on the bopy ligand. Accordingly, the HOMO − 1 → LUMO transition can be seen as mixed Re → bopy (MLCT) and Cl → bopy (LLCT) or a delocalized MLLCT (metal–ligand-to-ligand CT) description can be used.

The experimental absorption bands at 300.0 and 220.2 nm are attributed to *metal-to-ligand charge transfer* (occurring from the rhenium ion to the π-antibonding orbitals of the bopy ligand or π-antibonding orbitals of the carbonyl group), *ligand–ligand charge transfer* and intraligand (IL) transitions (Table 3).

5. Supplementary material

CCDC 638024 contains the supplementary crystallographic data for $C_{15}H_9ClNO_4Re$. These data can be obtained free of charge via http://www.ccdc.cam.ac.uk/conts/retrieving.html, or from the Cambridge Crystallographic Data Centre, 12 Union Road, Cambridge CB2 1EZ, UK; fax: (+44) 1223-336-033; or e-mail: deposit@ccdc.cam.ac.uk.

Table 3
The energy and molar absorption coefficients of experimental absorption bands and the electronic transitions calculated with the TDDFT method for **1**

The most important orbital excitations	Character	λ [nm]	E [eV]	f	Experimental λ [nm] (E [eV]) ε
H − 1 → L	d/π(Cl) → π^*(bopy)	540.4	2.29	*0.0041*	486.3.(2.55) 9440
H − 1 → L	d/π(Cl) → π^*(bopy)	491.8	2.52	*0.1499*	
H − 3 → L	π(bopy) → π^*(bopy)	361.5	3.43	*0.0123*	300.0 (4.13) 32500
H − 4 → L	π(bopy)/π(Cl) → π^*(bopy)	341.2	3.63	*0.2379*	
H − 6 → L	π(bopy)/π(Cl)/d → π^*(bopy)	315.4	3.93	*0.0263*	
H − 1 → *L* + 1	d/π(Cl) → π^*(bopy)	312.3	3.97	*0.0433*	
H − 7 → L	π(bopy)/π(Cl) → π^*(bopy)	279.1	4.44	*0.0906*	220.2 (5.63) 77700
H → *L* + 2	d/π(Cl) → π^*(bopy)	269.2	4.61	*0.0288*	
H − 1 → *L* + 2	d/π(Cl) → π^*(bopy)	266.9	4.65	*0.0227*	
H − 1 → *L* + 2	d/π(Cl) → π^*(bopy)	265.4	4.67	*0.0326*	
H − 8 → L	σ(Cl)/π(bopy) → π^*(bpzpy)	261.8	4.74	*0.0205*	
H − 2 → *L* + 3	d/π(O) → π^*(CO)	259.9	4.77	*0.1094*	
H − 4 → *L* + 1	π(bopy)/π(Cl) → π^*(bopy)	242.5	5.11	*0.0247*	
H − 5 → *L* + 1	π(Cl)/π(bopy)/d → π^*(bopy)	229.4	5.41	*0.0983*	
H − 2 → *L* + 6	d/π(O) → π^*(CO)	222.7	5.57	*0.0581*	
H − 4 → *L* + 2	π(bopy)/π(Cl) → π^*(bopy)	212.5	5.83	*0.0480*	
H − 7 → *L* + 1	π(bopy)/π(Cl) → π^*(bopy)	209.7	5.91	*0.0409*	
H − 1 → *L* + 9	d/π(Cl) → π^*(CO)/π^*(bopy)	203.5	6.09	*0.0254*	
H − 5 → *L* + 2	π(Cl)/π(bopy)/d → π^*(bopy)	202.6	6.12	*0.0324*	
H − 4 → *L* + 4	π(Cl)/π(bopy) → π^*(CO)	201.6	6.15	*0.0205*	
H → *L* + 10	d/π(Cl) → π^*(CO)/π^*(bopy)	200.8	6.18	*0.0294*	
H − 8 → *L* + 1	σ(Cl)/π(bopy) → π^*(bpzpy)	200.0	6.20	*0.0546*	
H − 2 → *L* + 8	d/π(Cl) → π^*(CO)/π^*(bopy)	198.1	6.26	*0.0667*	
H − 14 → L	π(bopy) → π^*(bopy)	194.9	6.36	*0.1373*	
H − 2 → *L* + 9	d/π(O) → π^*(CO)/π^*(bopy)	194.6	6.37	*0.0567*	
H − 4 → *L* + 5	π(bopy)/π(Cl) → π^*(bopy)	193.0	6.42	*0.1552*	
H → *L* + 13	d/π(Cl) → π^*(CO)	190.3	6.51	*0.0822*	
H − 7 → *L* + 2	π(bopy)/π(Cl) → π^*(bopy)	188.6	6.57	*0.1763*	
H − 8 → *L* + 3	σ(Cl)/π(bopy) → π^*(CO)	187.8	6.60	*0.0403*	
H − 14 → L	π(bopy) → π^*(bopy)	187.1	6.63	*0.1449*	
H − 14 → L H − 3 → *L* + 5	π(bopy) → π^*(bopy)	186.5	6.65	*0.1216*	
H − 7 → *L* + 4	π(bopy)/π(Cl) → π^*(CO)	186.0	6.67	*0.1004*	
H − 6 → *L* + 5	π(bopy)/π(Cl) → π^*(bopy)	185.4	6.69	*0.0330*	
H − 8 → *L* + 3	σ(Cl)/π(bopy) → π^*(CO)	185.2	6.69	*0.1401*	

Acknowledgement

Crystallographic part was financed by funds allocated by the Ministry Science and Higher Education to the Institute of General and Ecological Chemistry, Technical University of Łódź.

References

[1] V. Balzani, A. Juris, M. Venturi, S. Campagna, S. Serroni, Chem. Rev. 96 (1996) 759.

[2] D.J. Stufkens, A. Vlček Jr., Coord. Chem. Rev. 177 (1998) 127.

[3] I.R. Farrell, A. Vlček Jr., Coord. Chem. Rev. 208 (2000) 87.

[4] A. Vogler, H. Kunkely, Coord. Chem. Rev. 200–202 (2000) 991.

[5] D.R. Striplin, G.A. Crosby, Coord. Chem. Rev. 211 (2001) 163.

[6] A. Vlček Jr., M. Busby, Coord. Chem. Rev. 250 (2006) 1755.

[7] S. Ranjan, S.-Y. Li, K.-C. Hwang, W.-L. Ching, C.-S. Liu, Y.-T. Tao, C.-H. Chien, S.-M. Peng, G.-H. Lee, Inorg. Chem. 42 (2003) 1248.

[8] F. Li, G. Cheng, Y. Zhao, J. Feng, S. Liu, M. Zhang, Y. Ma, J. Shen, Appl. Phys. Lett. 83 (2003) 4716.

[9] P. Christensen, A. Hamnett, A.V.G. Muir, J.A. Timney, J. Chem. Soc., Dalton Trans. (1992) 1455.

[10] H. Hori, F.P.A. Johnson, K. Koike, K. Takeuchi, T. Ibusuki, O. Ishitani, J. Chem. Soc., Dalton Trans. (1997) 1019.

[11] S.S. Jurisson, J.D. Lydon, Chem. Rev. 99 (1999) 2205.

[12] W.A. Volkert, T.J. Hoffman, Chem. Rev. 99 (1999) 2269.

[13] W. Kaim, B. Schwederski, O. Heilmann, F.M. Hornung, Coord. Chem. Rev. 182 (1999) 323.

[14] S.B. Jiménez-Pulido, M. Sieger, A. Knödler, O. Heilmann, M. Wanner, B. Schwederski, J. Fiedler, M.N. Moreno-Carretero, W. Kaim, Inorg. Chim. Acta 325 (2001) 65.

[15] H. Chermette, Coord. Chem. Rev. 178–180 (1998) 699.

[16] STOE & Cie, X-RED. Version 1.18. STOE & Cie GmbH, Darmstadt, Germany, 1999.

[17] G.M. Sheldrick, Acta Crystallogr., Sect. A 46 (1990) 467.

[18] G.M. Sheldrick, SHELXL97. Program for the Solution and Refinement of Crystal Structures, University of Göttingen, Germany, 1997.

[19] G.M. Sheldrick, SHELXTL: release 4.1 for Siemens Crystallographic Research Systems, 1990.

[20] M.J. Frisch, G.W. Trucks, H.B. Schlegel, G.E. Scuseria, M.A. Robb, J.R. Cheeseman, J.A. Montgomery Jr., T. Vreven, K.N. Kudin, J.C. Burant, J.M. Millam, S.S. Iyengar, J. Tomasi, V. Barone, B. Mennucci, M. Cossi, G. Scalmani, N. Rega, G.A. Petersson, H. Nakatsuji, M. Hada, M. Ehara, K. Toyota, R. Fukuda, J. Hasegawa, M. Ishida, T. Nakajima, Y. Honda, O. Kitao, H. Nakai, M. Klene, X. Li, J.E. Knox, H.P. Hratchian, J.B. Cross, C. Adamo, J. Jaramillo, R. Gomperts, R.E. Stratmann, O. Yazyev, A.J. Austin, R. Cammi, C. Pomelli, J.W. Ochterski, P.Y. Ayala, K. Morokuma, G.A. Voth, P. Salvador, J.J. Dannenberg, V.G. Zakrzewski, S. Dapprich, A.D. Daniels, M.C. Strain, O. Farkas, D.K. Malick, A.D.

Rabuck, K. Raghavachari, J.B. Foresman, J.V. Ortiz, Q. Cui, A.G. Baboul, S. Clifford, J. Cioslowski, B.B. Stefanov, G. Liu, A. Liashenko, P. Piskorz, I. Komaromi, R.L. Martin, D.J. Fox, T. Keith, M.A. Al-Laham, C.Y. Peng, A. Nanayakkara, M. Challacombe, P.M.W. Gill, B. Johnson, W. Chen, M.W. Wong, C. Gonzalez, J.A. Pople, GAUSSIAN 03, Revision B.03, Gaussian, Inc., Pittsburgh, PA, 2003.
[21] A.D. Becke, J. Chem. Phys. 98 (1993) 5648.
[22] C. Lee, W. Yang, R.G. Parr, Phys. Rev. B 37 (1988) 785.
[23] M.E. Casida, in: J.M. Seminario (Ed.), Recent developments and applications in modern density functional theory, Theoretical and Computational Chemistry, vol. 4, Elsevier, Amsterdam, 1996.
[24] P.C. Hariharan, J.A. Pople, Theor. Chim. Acta 28 (1973) 213.
[25] V.A. Rassolov, M.A. Ratner, J.A. Pople, P.C. Redfern, L.A. Curtiss, J. Comp. Chem. 22 (2001) 976.
[26] P.J. Hay, W.R. Wadt, J. Chem. Phys. 82 (1985) 299.
[27] K. Eichkorn, F. Weigend, O. Treutler, R. Ahlrichs, Theor. Chem. Acc. 97 (1997) 119.
[28] P.J. Giordano, M.S. Wrighton, J. Am. Chem. Soc. 101 (1979) 2888.
[29] K. Nakamoto, Infrared and Raman Spectra of Inorganic and Coordination Compounds, fourth ed., Wiley Interscience, New York, 1986.
[30] C.A. Hunter, J.K.M. Sanders, J. Am. Chem. Soc. 112 (1990) 5525.